Asymmetrical Hybrid Optical OFDM for Visible Light Communications With Dimming Control

Qi Wang, Zhaocheng Wang, Senior Member, IEEE, and Linglong Dai, Senior Member, IEEE

Abstract—This letter proposes an asymmetrical hybrid optical orthogonal frequency division multiplexing (AHO-OFDM) scheme for dimmable visible light communication systems. In the proposed scheme, either asymmetrically clipped optical OFDM (ACO-OFDM) or pulse-amplitude-modulated discrete multitone (PAM-DMT) signal is inverted and then both the signals are combined for transmission, where pulsewidth modulation is no longer required for dimming control. The power of ACO-OFDM and PAM-DMT signals is adjusted so that the amplitude of the combined AHO-OFDM signal is asymmetrical, which could utilize all the available subcarriers as well as the entire dynamic range of light-emitting diodes with various dimming levels. Simulation results show that the proposed scheme could achieve a wide dimming range with a small throughput fluctuation.

Index Terms—Orthogonal frequency division multiplexing (OFDM), visible light communication (VLC), dimming control, light emitting diode (LED).

I. Introduction

IGHT emitting diodes (LEDs) have been emerging as a promising technology to replace incandescent or fluorescent lamps due to their distinct advantages such as long lifetime, high efficiency, small size, and low power consumption. Motivated by the dramatic development of LED technologies and the scarce wireless spectrum, visible light communication (VLC) is gaining constantly increasing attention in academia and industry. Features like worldwide usage, unregulated bandwidth, low cost, and guaranteed security make VLC a promising candidate to complement the conventional radio frequency counterpart [1], [2]. Recently, orthogonal frequency division multiplexing (OFDM) has been employed in VLC systems due to its resistance to inter-symbol interference (ISI) and high spectral efficiency, where the OFDM baseband signal is used to modulate the instantaneous power of the optical emitter [3]. In order to maintain the actual signal realvalued and non-negative, several optical OFDM methods have been proposed such as DC biased

Manuscript received January 15, 2015; revised February 5, 2015; accepted February 16, 2015. Date of publication February 20, 2015; date of current version April 8, 2015. This work was supported in part by the National Key Basic Research Program of China under Grant 2013CB329203, in part by the National Nature Science Foundation of China under Grant 61271266, in part by the Shenzhen Visible Light Communication System Key Laboratory under Grant ZDSYS20140512114229398, and in part by the Shenzhen Peacock Plan under Grant 1108170036003286.

The authors are with the Tsinghua National Laboratory for Information Science and Technology, Department of Electronic Engineering, Tsinghua University, Beijing 100084, China (e-mail: qiwang11@mails.tsinghua.edu.cn; zcwang@tsinghua.edu.cn; daill@tsinghua.edu.cn).

Color versions of one or more of the figures in this letter are available online at http://ieeexplore.ieee.org.

Digital Object Identifier 10.1109/LPT.2015.2404972

OFDM (DCO-OFDM), asymmetrically clipped optical OFDM (ACO-OFDM), pulse-amplitude-modulated discrete multitone (PAM-DMT), and hybrid ACO-OFDM (HACO-OFDM) [4]–[8].

In indoor VLC systems, the brightness of LED light should be dimmed for the convenience of illumination [9]. Furthermore, dimming technology is energy efficient and provides high-quality color performance [10]. For single carrier pulsed modulations such as on-off keying (OOK) and pulse-position modulation (PPM), dimming could be achieved by changing either the pulse intensity or the duty cycle of pulse width modulation (PWM) and some coding schemes have been proposed [11], [12]. Conventional optical OFDM schemes concentrate mainly on data transmission and could not support dimming control efficiently. Several dimming techniques have been proposed for OFDM-based VLC systems. In [13], the light is dimmed by adjusting the duty cycle of the pulse width for each time-domain signal, where extremely high-frequency pulse width modulation (PWM) signals are required for high speed transmission and it is not preferred for practical implementation. In [14], the OFDM signals are only modulated onto the PWM signals during the on-state, which requires a relatively low-frequency PWM signal but leads to the reduction of data rate.

contribution, asymmetrical hybrid optical OFDM (AHO-OFDM) is proposed for visible light communication systems, which fully exploits the subcarriers and the dynamic range of LEDs for supporting various dimming targets in order to enhance the achievable system performance. Since different dimming targets require different DC bias, only asymmetrical signals could fully utilize the dynamic range of LEDs. Our proposed scheme combines ACO-OFDM signals occupying odd subcarriers and PAM-DMT signals using even subcarriers in the time domain, where either ACO-OFDM signal or PAM-DMT signal is inverted and the power of both the signals is adjusted to make the combined signal asymmetrical. The combined bipolar signal is then biased according to different dimming requirements to guarantee that the transmitted signal is non-negative. Our simulation results demonstrate its ability to achieve a wide dimming range with a small throughput fluctuation.

II. OFDM-BASED VLC SYSTEM

For OFDM-based VLC system with N subcarriers, the transmitted bit stream is mapped onto the complex-valued symbols, X_k , $k=1,2,\cdots,N-1$, according to the chosen modulation scheme, such as PAM or quadrature amplitude modulation (QAM). Hermitian symmetry is imposed on the OFDM subcarriers to guarantee that the timedomain signals are real-valued, where we have $X_k = X_{N-k}^*$,

 $k=1,2,\cdots,N/2-1$, and the 0-th as well as the N/2-th subcarriers are set to zero. The time-domain OFDM signal is then obtained by the inverse fast Fourier transform (IFFT) as

$$x_n = \frac{1}{\sqrt{N}} \sum_{k=0}^{N-1} X_k \exp\left(j\frac{2\pi}{N}nk\right), \quad n = 0, 1, \dots, N-1.$$
 (1)

In DCO-OFDM, a DC bias is added to x_n to make sure that the transmitted signal is non-negative. In ACO-OFDM and PAM-DMT, only the odd subcarriers or the imaginary part of the subcarriers are modulated so that the time-domain signal follows a half-wave symmetry [5], [6]. Therefore, the bipolar OFDM signals could be directly clipped at zero without any information loss. In HACO-OFDM, ACO-OFDM signals occupying odd subcarriers and PAM-DMT signals using even subcarriers are directly added in the time domain and DC bias is not required. Cyclic prefix (CP) is inserted at the beginning of each OFDM symbol to eliminate the ISI. After that, the signal is parallel to serial (P/S) converted into a signal stream for modulating LEDs.

At the receiver, the optical signal is detected by avalanche photodiodes and converted to the electronic signal. Both shot-noise and thermal-noise are introduced at the receiver, which may be modeled as additive white Gaussian noise (AWGN) [15]. After serial-to-parallel (S/P) conversion and CP removal, the received signals r_n , $n = 0, 1, \dots, N-1$, are then transformed to the frequency domain by fast Fourier transform (FFT)

$$R_k = \frac{1}{\sqrt{N}} \sum_{n=0}^{N-1} r_n \exp\left(-\frac{j2\pi kn}{N}\right), \quad k = 0, 1, \dots, N-1,$$
(2)

which are thereafter used for signal demodulation.

III. PROPOSED AHO-OFDM

The conventional optical OFDM schemes concentrate only on data transmission and could not support various dimming levels efficiently. To maintain the high spectral efficiency and support dimming control at the same time, a novel AHO-OFDM scheme is proposed in this section.

In AHO-OFDM, ACO-OFDM and PAM-DMT signals are combined to transmit simultaneously. In PAM-DMT, only the imaginary part of even subcarriers is modulated to make sure that the ACO-OFDM symbols are not interfered. Unlike the scheme in [7] where ACO-OFDM and PAM-DMT signals are directly added, either ACO-OFDM or PAM-DMT signal is inverted in AHO-OFDM so that the combined signals are bipolar. Dimming control is achieved by directly adjusting the amplitude of the combined signals so that PWM signal is not required. Given different powers of ACO-OFDM and PAM-DMT signals, the powers of positive and negative signals are unequal, which makes the combined AHO-OFDM signals asymmetrical and therefore the dynamic range of LEDs could be fully utilized. The combined signals are biased by $I_{\rm bias}$ and the transmitted AHO-OFDM signals generated

by ACO-OFDM and inverse PAM-DMT are given by

$$z_n = x_{\text{ACO},n} - y_{\text{PAM},n} + I_{\text{bias}}, \quad n = 0, 1, \dots, N - 1,$$
 (3)

where $x_{ACO,n}$ and $y_{PAM,n}$ denote the time-domain signals of ACO-OFDM and PAM-DMT, respectively.

According to the central limit theorem, the time-domain OFDM signal in (1) approximates a Gaussian distribution when $N \ge 64$ [15]. In ACO-OFDM, the negative signals are directly clipped at zero. Therefore, the distribution of $x_{ACO,n}$ could be written as [16]

$$p_{\text{ACO}}(x_{\text{ACO},n}) = \begin{cases} \frac{1}{2}, & x_{\text{ACO},n} = 0; \\ \frac{1}{\sqrt{2\pi}\sigma_{\text{ACO}}} & \exp\left(-\frac{x_{\text{ACO},n}^2}{2\sigma_{\text{ACO}}^2}\right), & x_{\text{ACO},n} > 0, \end{cases}$$
(4)

where σ_{ACO} denotes the root mean square (RMS) of the unclipped ACO-OFDM signal. The expectation of $x_{ACO,n}$ is then calculated by $E\left(x_{ACO,n}\right) = \sigma_{ACO}/\sqrt{2\pi}$ [17], [18].

Similar to ACO-OFDM, the distribution of PAM-DMT signals $p_{\text{PAM}} \left(y_{\text{PAM},n} \right)$ could be calculated and the expectation of the time-domain signal $y_{\text{PAM},n}$ is given by $E \left(y_{\text{PAM},n} \right) = \sigma_{\text{PAM}} / \sqrt{2\pi}$, where σ_{PAM} denotes the RMS of the unclipped PAM-DMT signal. The average amplitude of the combined AHO-OFDM signal can be calculated as

$$I_D = E(z_n) = \frac{\sigma_{\text{ACO}}}{\sqrt{2\pi}} - \frac{\sigma_{\text{PAM}}}{\sqrt{2\pi}} + I_{\text{bias}}, \tag{5}$$

which is proportional to the average optical power of LEDs since the amplitude of AHO-OFDM signal is used to modulate the instantaneous power of the optical emitter.

Due to the nonlinear transfer characteristics of LEDs, the transmitted time-domain signal is constrained in a limited range. We denote I_H and I_L as the maximum and minimum allowed signals according to current levels permitted by LEDs. The dimming level η is defined as

$$\eta = (I_D - I_L) / (I_H - I_L). \tag{6}$$

For a given dimming level η , the average amplitude I_D can be obtained according to (6). It is seen from (5) that the average amplitude I_D is determined by the DC bias $I_{\rm bias}$ as well as $\sigma_{\rm ACO}$ and $\sigma_{\rm PAM}$. Since the amplitude of combined AHO-OFDM signal is constrained by the dynamic range of LEDs, it has to be clipped when it is beyond the dynamic range of LEDs, which results in undesirable clipping distortion. To estimate the clipping distortion of the proposed scheme, we define the scaling factors of ACO-OFDM and PAM-DMT as $\beta_{\rm ACO}$ and $\beta_{\rm PAM}$, where we have $\beta_{\rm ACO} = (I_H - I_{\rm bias})/\sigma_{\rm ACO}$ and $\beta_{\rm PAM} = (I_{\rm bias} - I_L)/\sigma_{\rm PAM}$. The probability of the clipped signal is then given by

$$P(z_{n} > I_{H}) = P(x_{ACO,n} - y_{PAM,n} > I_{H} - I_{bias})$$

$$= \int_{0}^{\infty} p_{PAM}(y) \int_{\beta_{ACO}\sigma_{ACO} + y}^{\infty} p_{ACO}(x) dx dy,$$
(7)

and

$$P(z_{n} < I_{L}) = P\left(y_{\text{PAM},n} - x_{\text{ACO},n} > I_{\text{bias}} - I_{L}\right)$$

$$= \int_{0}^{\infty} p_{\text{ACO}}(x) \int_{\beta_{\text{PAM}} \sigma_{\text{PAM}} + x}^{\infty} p_{\text{PAM}}(y) \, dy dx.$$
(8)

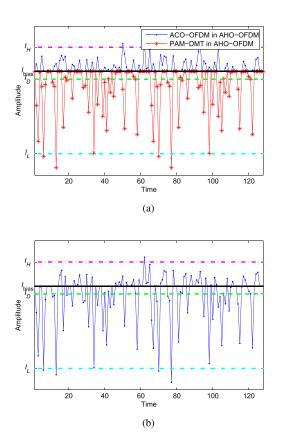


Fig. 1. An example of AHO-OFDM signal with dimming level $\eta=70\%$. (a) ACO-OFDM and PAM-DMT signals in AHO-OFDM. (b) The combined AHO-OFDM signal.

When the scaling factors β_{ACO} and β_{PAM} are large enough, the probability of clipped signal would be very small and clipping distortion can be suppressed. For example, in the case of $\beta_{ACO} = \beta_{PAM} = 3$, the probability of the clipped signal would be less than 1%. However, a large scaling factor will result in low effective power at the receiver, which degrades the system performance [4]. Therefore, a trade-off has to be made between the effective power and the clipping distortion for a required bit error rate (BER) performance. When the scaling factors are chosen, the required DC bias for the desired dimming level η can be derived as

$$I_{\text{bias}} = \frac{\beta_{\text{ACO}}\beta_{\text{PAM}}\sqrt{2\pi} \left((I_H - I_L) \eta + I_L \right) - \beta_{\text{ACO}}I_L - \beta_{\text{PAM}}I_H}{\beta_{\text{ACO}}\beta_{\text{PAM}}\sqrt{2\pi} - \beta_{\text{ACO}} - \beta_{\text{PAM}}}$$
(9)

according to the definition of scaling factors and (5)-(6).

Figure 1 illustrates an example of AHO-OFDM signal generated by ACO-OFDM and inverse PAM-DMT, where the required dimming level is 70% and the number of subcarriers is set to 128. 16QAM and 16PAM are employed in ACO-OFDM and PAM-DMT, respectively. The scaling factors of both ACO-OFDM and PAM-DMT are set to 3. In Fig. 1(a), the ACO-OFDM and inverse PAM-DMT signals are depicted separately, where the former is above the DC bias I_{bias} and the latter is below it. Figure 1(b) shows the combined AHO-OFDM signals, which are asymmetrical to the

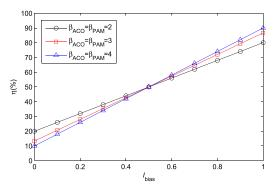


Fig. 2. Optical dimming level η as a function of β_{ACO} , β_{PAM} , and I_{bias} .

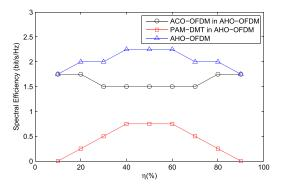


Fig. 3. The achievable spectral efficiency in AHO-OFDM with different dimming levels.

DC bias I_{bias} . We can see that I_{bias} is unequal to the desired average amplitude I_D and the dynamic range of LEDs could be fully utilized.

IV. SIMULATION RESULTS

Simulations were conducted to evaluate the performance of the proposed AHO-OFDM scheme. The maximum and minimum allowed signals of LEDs were set as $I_H=1$ and $I_L=0$, respectively. Figure 2 shows the obtained dimming level η as a function of $\beta_{\rm ACO}$, $\beta_{\rm PAM}$, and $I_{\rm bias}$ according to (9). It can be seen that a wide dimming range is achieved by the proposed scheme. For example, when the scaling factors $\beta_{\rm ACO}=\beta_{\rm PAM}=4$, the achieved dimming range is from 10% to 90%. It is notable that the dimming level can be further increased if we increase the scaling factors. When the required dimming level is very low or high, we could use larger scaling factors to support a wider dimming range. Therefore, the proposed scheme could achieve arbitrary dimming range in theory.

For a target BER of 2×10^{-3} and a relatively high noise power of $-10\,\mathrm{dBm}$, Fig. 3 depicts the achievable spectral efficiency in AHO-OFDM with different dimming levels, where QAM and PAM are employed in ACO-OFDM and PAM-DMT, respectively. Since different dimming levels require different DC biases, the dynamic ranges of ACO-OFDM and PAM-DMT are also different in AHO-OFDM, which result in different SNRs at the receiver. In order to achieve a target BER, the modulation orders should be adaptive to different SNRs. For example, when the dimming level is 50%, 64QAM and 8PAM are

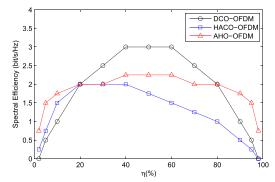


Fig. 4. The achievable spectral efficiency comparison of AHO-OFDM, DCO-OFDM and HACO-OFDM with different dimming levels.

used for ACO-OFDM and PAM-DMT, respectively. However, the modulations are 64QAM and 4PAM for ACO-OFDM and PAM-DMT when the dimming level is reduced to 30%. Besides, it can be seen in Fig. 2 that a larger scaling factor should be used to achieve a wider dimming range. Therefore, the scaling factors should also be adjusted for different dimming levels. We set the scaling factor as 3 when the dimming level is between 20% and 80%. When the desired dimming level is beyond the range, the scaling factor should be increased to achieve a wider dimming range. PAM-DMT and inverse ACO-OFDM are employed when the dimming level $\eta > 50\%$ to achieve better performance since ACO-OFDM utilizing two dimensions could transmit more bits than PAM-DMT with the same power. It can be seen that the proposed scheme could support a wide dimming range with a small throughput fluctuation. Apart from the data transmitted by ACO-OFDM, our proposed scheme could offer extra data transmission by incorporating PAM-DMT.

The performance of AHO-OFDM is also compared with DCO-OFDM and HACO-OFDM. In DCO-OFDM, dimming control is achieved by simply adjusting the DC bias, which does not require PWM signals. Adaptive scaling factors can be used to realize different dimming levels in DCO-OFDM to mitigate clipping distortion. In the HACO-OFDM scheme, the optical power is equally distributed to ACO-OFDM and PAM-DMT, and a DC bias still has to be added when the required dimming level is high. The achievable spectral efficiency comparison of HACO-OFDM, DCO-OFDM and the proposed AHO-OFDM with different dimming levels are shown in Fig. 4. It can be seen that the proposed AHO-OFDM could support a much wider dimming range compared with its two counterparts, and its achievable spectral efficiency is relatively stable when the dimming level varies since its asymmetry could fully utilize the dynamic range of LEDs. For example, it could support a wide dimming range from 5% to 95% with the spectral efficiency of at least 1.5 bits/s/Hz. For a extremely small dimming level where DCO-OFDM and HACO-OFDM couldn't work, i.e., 2%, the achievable spectral efficiency is still 0.75 bits/s/Hz for AHO-OFDM. For a certain dimming level, the optical power of different schemes is the same. Therefore, the proposed scheme is more power efficient when the required dimming level is very high or very low since it could transmit more bits.

V. Conclusions

An improved modulation scheme called AHO-OFDM has been proposed for VLC systems, which fully exploits the subcarriers and entire dynamic range of LEDs for various dimming targets in order to enhance the performance. In the proposed scheme, ACO-OFDM and PAM-DMT signals are combined with different power levels and one of them is inverted to obtain asymmetrical OFDM signals. Therefore, PWM signal is not necessary, which reduces the implementation complexity. Simulation results have shown that the proposed AHO-OFDM based VLC system can support a wide dimming range with a small throughput fluctuation.

REFERENCES

- [1] A. Jovicic, J. Li, and T. Richardson, "Visible light communication: Opportunities, challenges and the path to market," *IEEE Commun. Mag.*, vol. 51, no. 12, pp. 26–32, Dec. 2013.
- [2] Q. Wang, Z. Wang, S. Chen, and L. Hanzo, "Enhancing the decoding performance of optical wireless communication systems using receiverside predistortion," *Opt. Exp.*, vol. 21, no. 25, pp. 30295–30305, Dec. 2013.
- [3] A. H. Azhar, T. Tran, and D. O'Brien, "A gigabit/s indoor wireless transmission using MIMO-OFDM visible-light communications," *IEEE Photon. Technol. Lett.*, vol. 25, no. 2, pp. 171–174, Jan. 15, 2013.
- [4] Z. Wang, Q. Wang, S. Chen, and L. Hanzo, "An adaptive scaling and biasing scheme for OFDM-based visible light communication systems," *Opt. Exp.*, vol. 22, no. 10, pp. 12707–12715, May 2014.
- [5] J. Armstrong and A. J. Lowery, "Power efficient optical OFDM," Electron. Lett., vol. 42, no. 6, pp. 370–372, Mar. 2006.
- [6] S. C. J. Lee, S. Randel, F. Breyer, and A. M. J. Koonen, "PAM-DMT for intensity-modulated and direct-detection optical communication systems," *IEEE Photon. Technol. Lett.*, vol. 21, no. 23, pp. 1749–1751, Dec. 1, 2009.
- [7] B. Ranjha and M. Kavehrad, "Hybrid asymmetrically clipped OFDM-based IM/DD optical wireless system," *IEEE/OSA J. Opt. Commun. Netw.*, vol. 6, no. 4, pp. 387–396, Apr. 2014.
- [8] Q. Wang, Z. Wang, and L. Dai, "Iterative receiver for hybrid asymmetrically clipped optical OFDM," *J. Lightw. Technol.*, vol. 32, no. 22, pp. 4471–4477, Nov. 15, 2014.
- [9] A. Tsiatmas, C. P. M. J. Baggen, F. M. J. Willems, J.-P. M. G. Linnartz, and J. W. M. Bergmans, "An illumination perspective on visible light communications," *IEEE Commun. Mag.*, vol. 52, no. 7, pp. 64–71, Jul. 2014.
- [10] I. Din and H. Kim, "Energy-efficient brightness control and data transmission for visible light communication," *IEEE Photon. Technol. Lett.*, vol. 26, no. 8, pp. 781–784, Apr. 15, 2014.
- [11] K. Lee and H. Park, "Modulations for visible light communications with dimming control," *IEEE Photon. Technol. Lett.*, vol. 23, no. 16, pp. 1136–1138, Aug. 15, 2011.
- [12] J. Kim and H. Park, "A coding scheme for visible light communication with wide dimming range," *IEEE Photon. Technol. Lett.*, vol. 26, no. 5, pp. 465–468, Mar. 1, 2014.
- [13] G. Ntogari, T. Kamalakis, J. Walewski, and T. Sphicopoulos, "Combining illumination dimming based on pulse-width modulation with visible-light communications based on discrete multitone," *IEEE/OSA J. Opt. Commun. Netw.*, vol. 3, no. 1, pp. 56–65, Jan. 2011.
- [14] Z. Wang, W.-D. Zhong, C. Yu, J. Chen, C. P. S. Francois, and W. Chen, "Performance of dimming control scheme in visible light communication system," *Opt. Exp.*, vol. 20, no. 17, pp. 18861–18868, Aug. 2012.
- [15] J. Armstrong, "OFDM for optical communications," J. Lightw. Technol., vol. 27, no. 3, pp. 189–204, Feb. 1, 2009.
- [16] X. Li, R. Mardling, and J. Armstrong, "Channel capacity of IM/DD optical communication systems and of ACO-OFDM," in *Proc.* IEEE Int. Conf. Commun. (IEEE ICC), Glasgow, U.K., Jun. 2007, pp. 2128–2133.
- [17] X. Li, J. Vucic, V. Jungnickel, and J. Armstrong, "On the capacity of intensity-modulated direct-detection systems and the information rate of ACO-OFDM for indoor optical wireless applications," *IEEE Trans. Commun.*, vol. 60, no. 3, pp. 799–809, Mar. 2012.
- [18] S. D. Dissanayake and J. Armstrong, "Comparison of ACO-OFDM, DCO-OFDM and ADO-OFDM in IM/DD systems," J. Lightw. Technol., vol. 31, no. 7, pp. 1063–1072, Apr. 1, 2013.